Astrochemistry: Recent Successes and Current Challenges
Proceedings IAU Symposium No. 231, 2005
D.C. Lis, G.A. Blake & E. Herbst, eds.
© 2005 International Astronomical Union
DOI: 00.0000/X000000000000000X

Spitzer observations of deeply obscured galactic nuclei

H.W.W. Spoon[1], J.V. Keane[2], J. Cami[3], F. Lahuis[4], A.G.G.M. Tielens[5], L. Armus[6], and V. Charmandaris[7]

[1]Cornell University, Astronomy Department, Ithaca, NY 14853, USA
email: spoon@astro.cornell.edu

[2] NASA Ames Research Center, MS 245-3, Moffett Field, CA 94035

[3] NASA Ames Research Center, MS 245-6, Moffett Field, CA 94035

[4] Leiden Observatory, P.O. Box 9513, 2300 RA Leiden, Netherlands

[5] SRON and Kapteyn Institute, P.O. Box 800, 9700 AV Groningen, The Netherlands

[6] Caltech, Spitzer Science Center, MS 220-6, Pasadena, CA 91125, USA

[7] Department of Physics, University of Greece, P.O. Box 2208, 71003 Heraklion, Greece

arXiv:astro-ph/0512037v1 1 Dec 2005

Abstract. We report on our first results from a mid-infrared spectroscopic study of ISM features in a sample of deeply obscured ULIRG nuclei using the InfraRed Spectrograph (IRS) on the Spitzer Space Telescope. The spectra are extremely rich and complex, revealing absorption features of both amorphous and crystalline silicates, aliphatic hydrocarbons, water ice and gas phase bands of hot CO and warm C_2H_2, HCN and CO_2. PAH emission bands were found to be generally weak and in some cases absent. The features are probing a dense and warm environment in which crystalline silicates and water ice are able to survive but volatile ices, commonly detected in Galactic dense molecular clouds, cannot. If powered largely by star formation, the stellar density and conditions of the gas and dust have to be extreme not to give rise to the commonly detected emission features associated with starburst.

Keywords. ISM: evolution – ISM: molecules – galaxies: ISM – galaxies: nuclei – infrared: ISM

1. Introduction

With the launch of the InfraRed Spectrograph (IRS) on the Spitzer Space Telescope, mid-infrared spectroscopists have been handed a powerful tool to study extragalactic objects at high signal-to-noise and over a wide mid-infrared wavelength range, previously only available for the study of Galactic sources and a few nearby galaxies.

The foundations for the Spitzer studies currently underway were laid by the Infrared Space Observatory (ISO), which freed mid-infrared spectroscopists from the confinements of the Earth's atmospheric windows and the atmosphere's glaring foreground emission.

Major extragalactic topics addressed early on in the ISO mission centered around the properties of dusty starbursts and how they evolve (e.g. Thornley et al. 2000), the unification of optically classified type 1 and 2 active galaxies in relation to the properties of the Active Galactic Nucleus (AGN) (e.g. Clavel et al. 2000; Laurent et al. 2000), and the dominant power source in Ultra-Luminous Infrared Galaxies (ULIRGs): massive starbursts or AGN activity (e.g. Genzel et al. 1998; Tran et al. 2001)?

After the expiration of ISO, two unusual galaxy spectra provided first mid-infrared insights into the properties of gas and dust in deeply obscured galactic nuclei. The 2–5 μm spectrum of the nucleus of NGC 4945 revealed strong absorptions of water ice (3 μm), CO_2 (4.26 μm) and a blend of 'XCN' and CO ice (4.65 μm), seen against a continuum obscuring the central massive black hole (Spoon et al. 2000). Groundbased follow-up

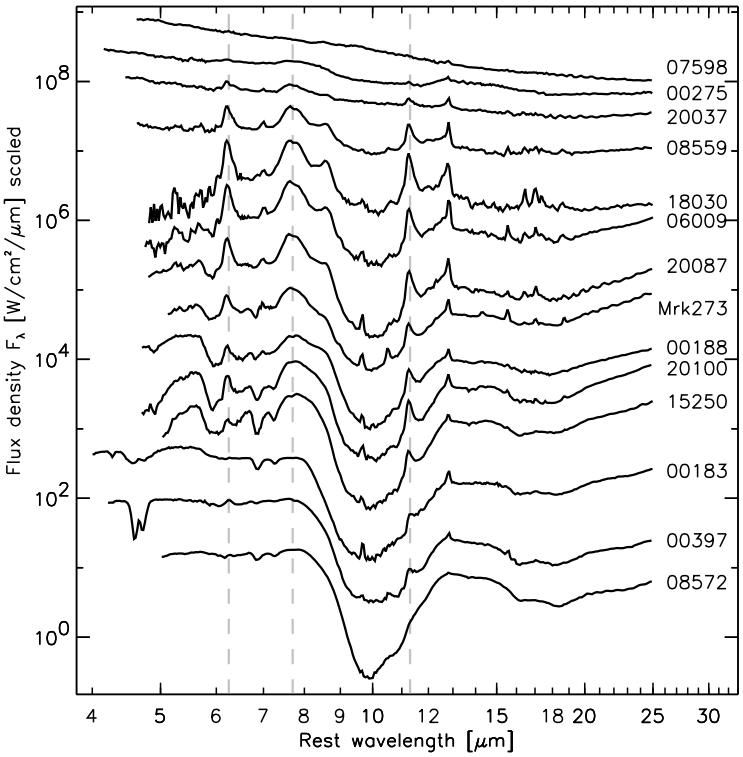

Figure 1. Spitzer IRS low-resolution spectra of ULIRGs sorted by spectral shape. The three spectra at the top are continuum-dominated (AGN-like), the next four are PAH-dominated (starburst-like) and the rest are absorption-dominated (burried nuclei). Vertical lines indicate the positions of the 6.2, 7.7 and 11.2 μm PAH emission bands

observations confirmed the 4.65 μm absorption band to consist of separate components of processed 'XCN' and CO ice and warm (35 K) CO gas. The detection of processed ices against the nuclear continuum is taken as an indication for the presence of dense star forming molecular clouds towards the nucleus of this active galaxy (Spoon et al. 2003).

The second unusual spectrum is that of the nucleus of NGC 4418, originally classified by Roche et al. (1986) as a "very extinguished galaxy", for its very deep 10 μm silicate absorption feature. Instead of the commonly detected PAH emission features, the 5.5–8 μm ISO spectrum of its nucleus is dominated by absorption features of water ice (6 μm), hydrocarbons (6.85 μm and 7.25 μm) and methane ice (7.67 μm), reminiscent of the line of sight towards our own Galactic Center (Spoon et al. 2001). Supporting groundbased observations indicate that most of the infrared luminosity ($L_{IR} = 10^{11}\,L_\odot$) from NGC 4418 is produced in a compact nucleus with a radius of less than 80 pc (Evans et al. 2003). If powered entirely by star formation, the conditions of the nuclear gas and dust within this environment must be exceptional not to give rise to emission features commonly associated with star formation.

A large scale follow-up study into the presence of 5.5–8 μm absorption features in ISO galaxy spectra resulted in the finding of 6 μm water ice absorption in 12 out of 19 ULIRGs, 2 out of 62 AGNs and 4 out of 21 starburst galaxies surveyed. Also, 6.85 μm hydrocarbon absorption was detected in three galaxies besides NGC 4418, all three of which are ULIRGs. The results are consistent with findings from other wavelength ranges

that more molecular material is present in ULIRG nuclei than in other galaxy types (Spoon et al. 2002).

In the following sections we present an overview of the first results from an IRS spectroscopic study of the properties of gas and dust in strongly obscured ULIRG nuclei. The spectra were selected from a larger sample of ULIRG spectra obtained as part of the GTO program of the Spitzer IRS team.

2. The diverse nature of the ULIRG family

Figure 1 offers a strikingly illustration of the diverse nature of the galaxies classified as ULIRGs. At the top of the figure we find ULIRG mid-infrared spectra dominated by AGN-heated hot dust, with IRAS 07598 displaying a weak silicate emission feature. Further down, the spectra of IRAS 20037 and IRAS 08559 show increasing contributions of PAH emission superimposed on the AGN continuum. Moving down to IRAS 18030 and IRAS 06009, PAH emission starts to dominate and silicate absorption at both 10 and 18 μm becomes apparent. In the spectrum of the next one down, IRAS 20087, the characteristic absorption edge of water ice at 5.7 μm starts to appear. The water ice feature deepens and the importance of PAH emission decreases moving down from Mrk 273 to IRAS 15250. At the same time, the depth of the 10 and 18 μm silicate features increases and hydrocarbons absorption bands at 6.85 and 7.25 μm become apparent. Further note how from IRAS 18030 to IRAS 15250 the characteristic PAH emission feature at 7.7 μm gradually gets replaced by a broad absorbed-continuum peak at 8 μm. Starburst diagnostics relying on the equivalent width or luminosity of the 7.7 μm PAH feature will have to carefully verify the nature of this peak (Spoon et al. 2004a). The bottom three spectra in figure 1 differ from those directly above by the presence of a strong near-infrared continuum and by the relative weakness of the 5.5–8 μm absorption features. Note how, due to the appreciable redshifts of IRAS 00183 and IRAS 00397, the IRS spectral coverage extends all the way down to rest frame 4 μm, facilitating the discovery of wide absorption features of CO gas in their spectra (Spoon et al. 2004b). Recent ground-based high-resolution M-band spectroscopy reveals the CO band to be also present in the spectrum of the low-redshift ULIRG IRAS 08572 (Geballe et al., in preparation).

3. Absorption features of crystalline silicates

We have detected significant substructure in the deep silicate absorption features towards a sample of strongly obscured ULIRG nuclei. The absorption features appear at 11, 16, 19, 23 and 28 μm and are best revealed by a spline fit to the amorphous silicate absorption component. We identify the residuals with crystalline silicates, most likely forsterite (Mg_2SiO_4). The clearest detection is offered by the spectrum of IRAS 08572, shown in detail in figure 2. This spectrum combines the deepest silicate feature in our sample with the complete absence of all commonly present PAH emission features. In figure 3 we show our 12 clearest crystalline silicate detections. For these we infer crystalline to amorphous silicate ratios of 7–15%, using the optical depth and opacities of the 10 μm amorphous and 16 μm crystalline band.

The detection of crystalline silicates appears to be geared to the more deeply enshrouded ULIRG spectra. While all 17 ULIRGs with $\tau(\mathrm{sil}) > 2.9$ do show the strong 16 μm feature, at lower silicate optical depth the number of detections of this band drops sharply. Between $\tau(\mathrm{sil})$=2.0 and $\tau(\mathrm{sil})$=2.9 only 1 out of 6 ULIRGs shows the feature and below that, only 3 out of 54. This also is apparent in the spectra shown in figure 1, in

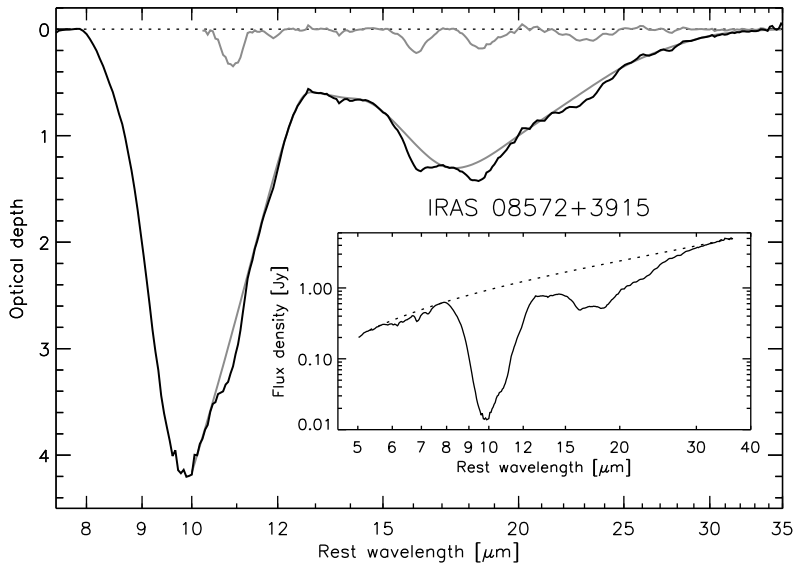

Figure 2. Silicate optical depth spectrum of IRAS 08572 (*black*) with a spline fit to the amorphous silicate component overplotted (*grey*). The residual spectrum, revealing crystalline features at 11, 16, 19 and 23 μm is shown in *grey* at the top of the plot. Inset: the 5–35 μm spectrum of IRAS 08572 with the adopted local continuum.

which the 16 μm feature can only be recognized in the spectra with the deepest silicate features.

The discovery of crystalline silicates in the ISM of ULIRGs stands in sharp contrast to the upper limit of 1% for the crystallinity of the Galactic ISM (Kemper et al. 2004, 2005). As stellar sources of silicate dust inject at least 5% of their silicates in crystalline form, the crystalline silicates arriving in the Galactic ISM must be rapidly transformed into amorphous silicates. The timescale for amorphization is estimated to be only 70 million years (Bringa et al., in preparation), considerably shorter than the timescale at which (crystalline) silicates are injected into the Galactic ISM (4 billion years; Bringa et al., in preparation). In ULIRGs and other mergers these time scales may be different. ULIRGs are characterized by a high rate of star formation driven by merging events. In contrast to the Galactic ISM, the enrichment of the dusty interstellar medium will be dominated by the rapidly evolving massive stars and the contribution by the more numerous low-mass stars will lag on the timescale associated with the ULIRG-merger event ($10^8 - 10^9$ yr; Murphy et al. 1996). Thus, we attribute the high fraction of crystalline silicates in these ULIRGs as compared to others to the relative 'youth' of these systems; e.g., the amorphitization process may lag the merger-triggered, star-formation-driven dust injection process. For a more detailed discussion on the discovery of crystalline silicates in ULIRG spectra we refer to Spoon et al. (2006).

4. Absorption features in the 5.5–8 μm range

The 5.5–8 μm spectral range of Galactic dense and diffuse ISM lines of sight is rich in absorption features of vibrational transitions of various molecular species which are diagnostics of the chemical and physical states of these environments (Chiar et al. 2000; Keane et al. 2001). Towards dense clouds, the profiles and strengths of the main volatile ice absorption bands of water ice (6.0 μm), NH_4^+ ice (6.85 μm) and methane ice (7.67 μm)

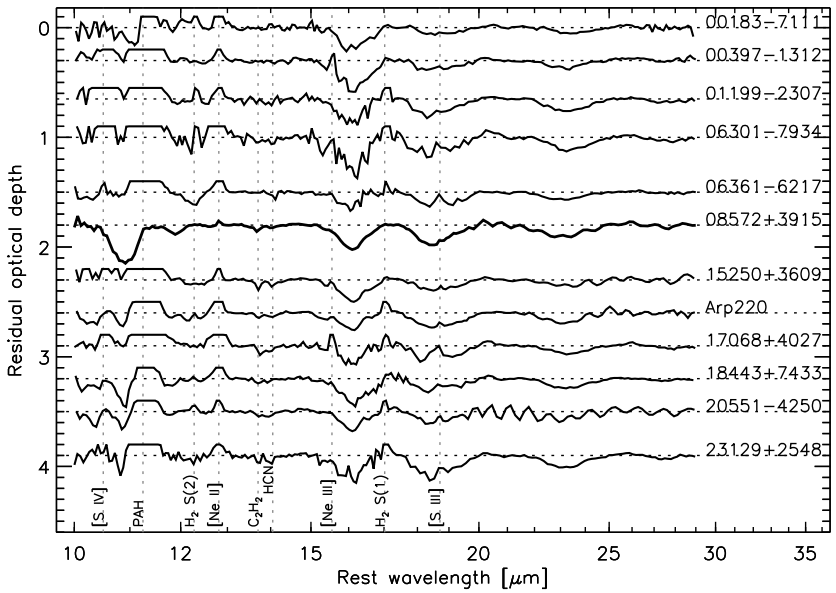

Figure 3. 10–30 μm residual optical depth spectra for 12 ULIRGs from our sample after subtraction of the amorphous silicate component. For plotting purposes, the spectra have been offset and truncated at residual optical depths of -0.1. Crystalline silicate features can be identified at 11, 16, 19, 23 and 28 μm

have been shown to vary considerably depending on the thermal history of the ice mantle. Observations of diffuse lines of sight, on the other hand, show absorption features in the 5.5–8 μm range that are associated with organic refractory dust: e.g. the C–H bending modes of aliphatic hydrocarbons at 6.85 and 7.25 μm as seen towards the Galactic Center (e.g. Chiar et al. 2000; Pendleton & Allamandola 2002). The strong detection by ISO of features of both the dense and the diffuse ISM towards several deeply enshrouded galactic nuclei (Spoon et al. 2001, 2002) has expanded the applicability of these diagnostics to external galaxies.

With the availability of IRS on Spitzer, both the wavelength coverage shortward of 5.7 μm and the spectral resolution in the 5.5–8 μm range have improved, enabling a better determination of the local continuum in this range, a clearer separation of the many spectral features and expansion of the study to a larger sample of galactic nuclei. Figure 4 shows the optical depth spectra for five deeply obscured merger nuclei. The top four spectra are dominated by strong absorption features centered at 6.0–6.1, 6.85 and 7.25 μm. Following earlier studies (e.g. Chiar et al. 2000; Spoon et al. 2001, 2002, 2004b), we identify the main components with water ice (6.0 μm) and the bending modes of C–H in aliphatic hydrocarbons (6.85 and 7.25 μm).

Compared to the top four spectra, the optical depth spectrum of Arp 220 (bottom panel) looks very different. Strong PAH emission bands at 5.70, 6.22 and 7.7 μm and emission lines of H_2 S(5) and [ArII] at 6.91 and 6.99 μm distort the otherwise pure absorption spectrum. While the two emission lines fill up the red wing of the 6.85 μm hydrocarbon band, the blue flank of the 7.7 μm PAH band overwhelms the 7.25 μm hydrocarbon band and the 6.22 μm PAH emission feature fills up the depth of the 6 μm water ice band. The same emission features are also weakly present in the spectrum of IRAS 15250, most notably the PAH emission feature at 6.22 μm. Evidently, the contribution of unconcealed star formation in IRAS 15250 is far smaller than in Arp 220.

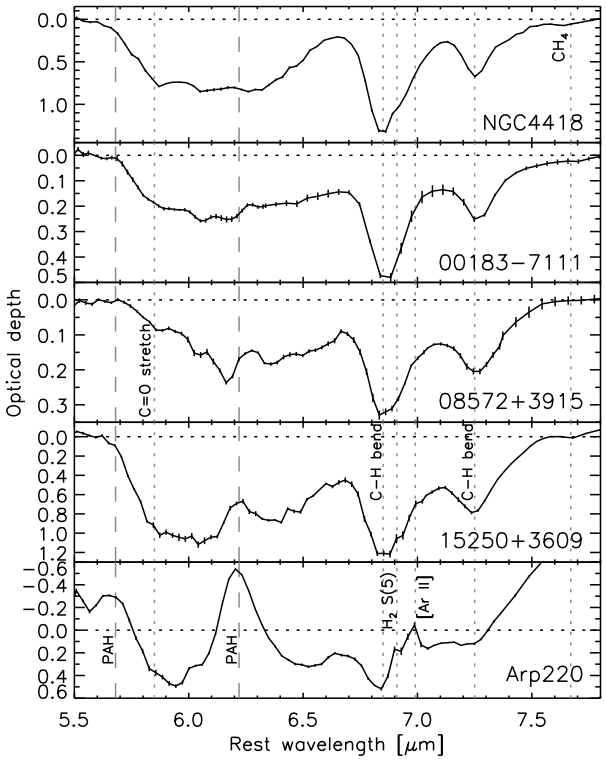

Figure 4. Optical depth spectra for five (U)LIRGs of absorption features in the 5.5–7.7 μm range. Vertical *dashed* lines denote the central wavelengths of PAH emission features at 5.7 and 6.22. Vertical *dotted* lines indicate the central positions of the C=O carbonyl stretch (5.88 μm), the C–H bending modes of hydrocarbons (6.85 and 7.25 μm), emission lines of H_2 S(5) (6.91 μm) and [ArII] (6.99 μm), and methane ice (7.67 μm)

At first glance, the spectral structure seen at 6.32 μm in the spectra of IRAS 08572 and IRAS 00183 appears to be the 6.22 μm PAH feature. However, neither the central wavelength nor the FWHM of the feature is consistent with an identification with interstellar 6.22 μm PAH. Instead, this feature may be 'carved out' by absorption bands of species absorbing in this range, like gas phase water or hydrocarbons. For a detailed study of the absorption features contributing to the 6 μm absorption complex we refer to Keane et al. (in preparation) and for a full analysis of the origin of the hydrocarbon bands in the spectrum of IRAS 08572 to Pendleton et al. (in preparation).

5. Absorption features of C_2H_2, HCN and CO_2

Using the high-resolution mode of IRS on Spitzer, we have discovered C_2H_2 (13.7 μm), HCN (14.03 μm) and CO_2 (15.0 μm) gas absorption features in the spectra of a number of deeply obscured ULIRG nuclei (Armus et al., in preparation). Our four clearest detections are shown in figure 5, together with excitation temperatures resulting from a preliminary, combined fit of the C_2H_2 and HCN profiles. The excitation temperatures found range from 150 K for Arp 220 to 400 K for IRAS 20100.

These features have previously been seen in ISO–SWS spectra of deeply embedded massive Young Stellar Objects (YSOs) (e.g. Lahuis & van Dishoeck 2000) and recently in the Spitzer spectra of a low mass YSO, IRS 46 (Lahuis et al., in prep.). In the massive

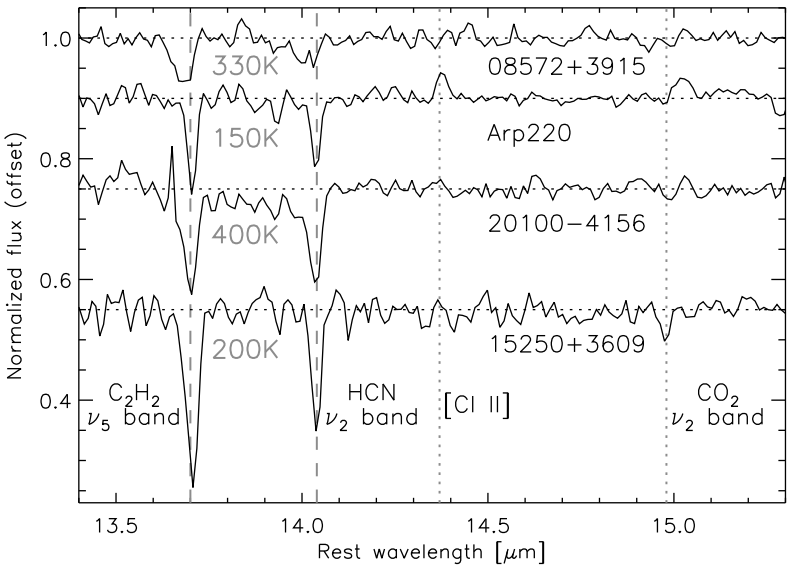

Figure 5. Continuum-normalized high-resolution IRS spectra of four deeply obscured ULIRGs. The spectra reveal the presence of gas absorption bands of C_2H_2 at 13.7 μm, HCN at 14.03 μm and CO_2 at 15.0 μm. Best fitting excitation temperatures for the C_2H_2 and HCN absorption bands are indicated on the plot. Also indicated is the [Cl II] line at 14.37 μm in Arp 220

YSOs, the features originate in the hot inner dense region of the shells surrounding the young stars. In the case of IRS 46 the features are believed to originate in the dense hot inner region of the protostellar disk. In these cases, the chemistry is dominated by evaporation of the molecules from the grains with subsequent gas-phase processing which enhances the abundances of C_2H_2 and HCN by orders of magnitude. Hence, C_2H_2 and HCN are typical tracers of high density ($> 10^8$ cm^{-3}) high temperature chemistry.

The detection of absorption features of C_2H_2, HCN and CO_2 in our ULIRGs might suggest the presence of a population of deeply embedded YSOs in their nuclear environments. However, an identification with embedded protostars is not supported by spectral evidence in other parts of our mid-infrared spectra (e.g. by the absence of commonly detected NH_4^+ ice at 6.85 μm and CO_2 ice at 15 μm; Gibb et al. 2004). In the light of other evidence present (e.g. interferometric detection of HCN in these nuclei; extreme compactness of the ultra-luminous sources; weakness of common starburst emission features such as PAHs and fine-structure lines of Neon and Sulphur), it seems more likely that the features arise from highly pressure-confined star formation in a dense medium — i.e. under star formation conditions more extreme than probed in ordinary starburst galaxies. This, and a more detailed analysis of the 13–15 μm features in ULIRG spectra, will be discussed in more detail in a future paper.

6. The 4.65 μm CO absorption feature

Absorption spectroscopy to study features of dust and gas in the 2–5 μm range requires the presence of a 2–5 μm background continuum source. Active galaxies, with a favorable orientation of their AGN, show AGN-heated hot dust in their spectra against which absorption features have been detected (e.g. Imanishi et al. 2002). Also some of the deeply obscured galactic nuclei reveal 2–5 μm absorption features against their near-infrared dust continua (e.g. UGC 5101: Imanishi et al. 2001; NGC 4945: Spoon et al.

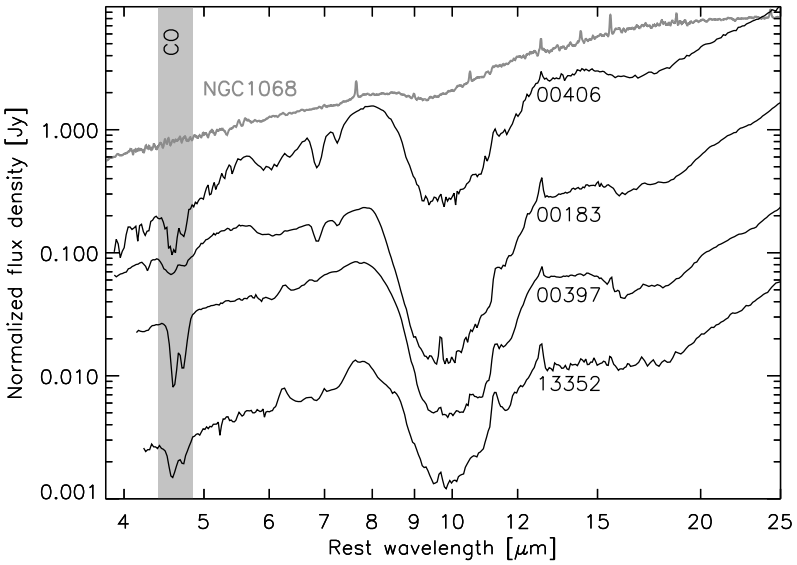

Figure 6. 4–25 μm spectra of four ULIRGs showing an absorption feature of gas phase CO at 4.65 μm. The spectra are compared to the ISO–SWS spectrum of the nucleus of the Seyfert-2 galaxy NGC 1068 (Sturm et al. 2000). The spectra have been scaled for plotting purposes

2000, 2003), while for other nuclei these are impossible to detect given the absence of a hot dust background source (e.g. NGC 4418: Spoon et al. 2001; or IRAS 15250: figure 1).

Here we report the first detection of strong absorption features of 4.65 μm gas phase CO in the spectra of four deeply obscured ULIRG nuclei with redshifts favorable to detection by Spitzer-IRS. The 4–25 μm spectra of the sources are compared in figure 6, their normalized flux profiles are shown in figure 7.

We have used the isothermal plane-parallel LTE gas models of Cami (Cami 2002) to model the CO gas absorption profile of IRAS 00183. A best fit to the observed profile is found for a model with a gas temperature of 720 K, a column density of $10^{19.5}$ cm^{-2} and an intrinsic line width of 50 km/s. The temperature is far higher than found toward Galactic ISM lines of sight, consistent with the clearly larger width of the feature compared to for instance Sgr A* (figure 7). Note that the density in the absorbing medium has to be high ($n > 3{\times}10^6$ cm^{-3}) to give rise to high J level absorption. This limits the size of the obscuring region to less than 0.03 pc (Spoon et al. 2004b). Similar fits for the CO profiles of the other three sources in figure 7 have not yet been made.

Following the discovery of hot CO gas in IRAS 00183, Lutz et al. (2004) have analyzed a sample of ISO AGN spectra for the presence of similar CO absorption features and found none to good limits. This suggests that the CO features seen in our ULIRG spectra do not arise in a typical AGN torus geometry, but rather are a signature of the special conditions in deeply obscured ULIRG nuclei — pointing to a fully covered rather than a torus geometry (Lutz et al. 2004).

7. Conclusions

Using the IRS spectrograph on the Spitzer Space Telescope, we have obtained mid-infrared spectra for a large sample of ULIRGs. The spectra show a great diversity in spectral shape, reflecting the diverse nature and merger evolutionary states of the sample.

Especially interesting for astrochemists is the subsample of spectra showing signatures

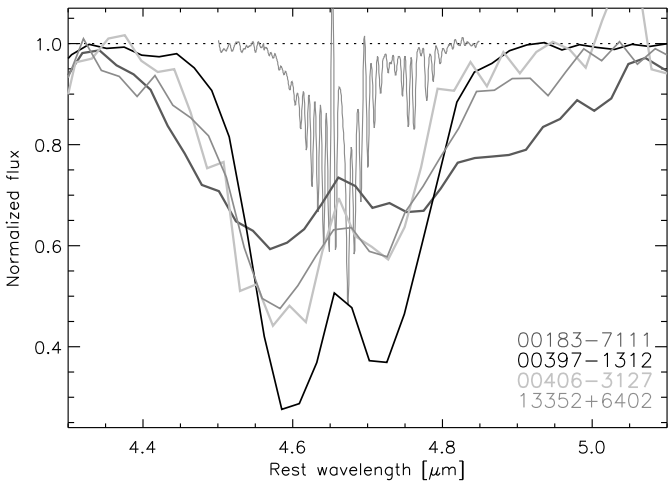

Figure 7. Comparison of the normalized flux profiles for the CO absorption features in the spectra of Sgr A* (*dark grey* narrow profile; Moneti et al. 2001) and the four ULIRGs shown in figure 6. Individual lines are resolved in the high-resolution ISO–SWS spectrum of Sgr A*

of strong obscuration, betraying the presence of huge amounts of dust and gas in and towards the merger nuclei. The wide spectral coverage of the IRS (5–38 μm), assisted by redshifts ranging from z=0.02 to z=0.4, allowed us to study the ISM in these sources from rest frame $\sim$3.8 μm to 37 μm, revealing absorption features of both amorphous and crystalline silicates, aliphatic hydrocarbons, water ice and gas phase bands of hot CO and warm C_2H_2, HCN and CO_2. PAH emission bands were found to be generally weak and in some cases absent.

Our analysis of the absorption features is far from complete and requires further comparison to the results from our emission line analysis to obtain a more detailed picture of the energetic processes responsible for these rich and complicated spectra. It is clear, however, at this time that the features are probing a dense and warm environment in which crystalline silicates and water ice are able to survive but volatile ices, commonly detected in Galactic dense molecular clouds, cannot. If powered largely by star formation, the stellar density and conditions of the gas and dust have to be extreme not to give rise to the commonly detected emission features associated with starburst.

Acknowledgements

Support for this work was provided by NASA through the Spitzer Space Telescope Fellowship Program, through a contract issued by the Jet Propulsion Laboratory, California Institute of Technology under a contract with NASA

References

Cami, J., 2002, Ph.D. thesis, Amsterdam Univ.
Clavel, J., Schulz, B., Altieri, B., et al., 2000, *A&A* 357, 839
Chiar, J.E., Tielens, A.G.G.M., Whittet, D.B.C., et al., 2000, *ApJ* 537, 749
Evans, A.S., Becklin, E.E., Scoville, N., et al., 2003, *AJ* 125, 2341
Genzel R., Lutz D., Sturm E., et al., 1998, *ApJ* 498, 579
Gibb, E.L., Whittet, D.C.B., Boogert, A.C.A., Tielens, A.G.G.M., 2004, *ApJS* 151, 35
Imanishi, M., Dudley, C.C., Maloney, P.R., 2001, *ApJ* 558, 93
Imanishi, M., 2002, *MNRAS* 319, 333

Keane, J.V., Tielens, A.G.G.M., Boogert, A.C.A., et al., 2001, *A&A* 376, 254
Kemper, F., Vriend, W.J., Tielens, A.G.G.M., 2004, *ApJ*, 609, 826
Kemper, F., Vriend, W.J., Tielens, A.G.G.M., 2005, *ApJ* 633, 534, erratum
Lahuis, F., van Dishoeck, E.F., 2000, *A&A* 355, 699
Laurent, O., Mirabel, I.F., Charmandaris, V., et al., 2000, *A&A* 359, 887
Lutz, D., Sturm, E., Genzel, R., et al., 2004, *A&A* 426, L5
Moneti, A., Cernicharo, J., Pardo, J.R., 2001, *ApJ* 549, L203
Murphy, T.W., Armus, L., Matthews, K., et al., 1996, *AJ*, 111, 1025
Pendleton, Y.J., Allamandola, L.J., 2002, *ApJS* 138, 75
Roche, P.F., Aitken, D.K., Smith, C.H., James, S.D., 1986, *MNRAS* 218, 19P
Spoon, H.W.W., Koornneef, J., Moorwood, A.F.M., et al., 2000, *A&A* 357, 898
Spoon, H.W.W., Keane, J.V., Tielens, A.G.G.M., et al., 2001, *A&A* 365, L353
Spoon, H.W.W., Keane, J.V., Tielens, A.G.G.M., et al., 2002, *A&A* 385, 1022
Spoon, H.W.W., Moorwood, A.F.M., Pontoppidan, K.M., et al., 2003, *A&A* 402, 499
Spoon, H.W.W., Moorwood, A.F.M., Lutz, D., et al. 2004a, *A&A* 414, 873
Spoon, H.W.W., Armus, L., Cami, J., et al., 2004b, *ApJS* 154, 184
Spoon, H.W.W., Tielens, A.G.G.M., Armus, L., et al., 2006, *ApJ* accepted (astro_ph/0509859)
Sturm, E., Lutz, D., Tran Q.D., et al., *A&A* 358, 481
Tran Q.D., Lutz D., Genzel R., et al., 2001, *ApJ* 552, 527
Thornley, M.D., Förster Schreiber, N.M., Lutz, D., et al., 2000, *ApJ* 539, 641